

## Direct self-heating power observations in pre-stressed piezoelectric actuators

Villalba Corbacho, Víctor; van Es, Johannes; Kuiper, Hans; Gill, Eberhard

**DOI**

[10.1016/j.sna.2021.113276](https://doi.org/10.1016/j.sna.2021.113276)

**Publication date**

2022

**Document Version**

Final published version

**Published in**

Sensors and Actuators A: Physical

**Citation (APA)**

Villalba Corbacho, V., van Es, J., Kuiper, H., & Gill, E. (2022). Direct self-heating power observations in pre-stressed piezoelectric actuators. *Sensors and Actuators A: Physical*, 333, Article 113276. <https://doi.org/10.1016/j.sna.2021.113276>

**Important note**

To cite this publication, please use the final published version (if applicable). Please check the document version above.

**Copyright**

Other than for strictly personal use, it is not permitted to download, forward or distribute the text or part of it, without the consent of the author(s) and/or copyright holder(s), unless the work is under an open content license such as Creative Commons.

**Takedown policy**

Please contact us and provide details if you believe this document breaches copyrights. We will remove access to the work immediately and investigate your claim.



# Direct self-heating power observations in pre-stressed piezoelectric actuators



Víctor Villalba Corbacho<sup>a,\*</sup>, Johannes van Es<sup>b</sup>, Hans Kuiper<sup>a</sup>, Eberhard Gill<sup>a</sup>

<sup>a</sup> Delft University of Technology, Kluyverweg 1, Delft, 2629 HS, Netherlands

<sup>b</sup> Royal Netherlands Aerospace Centre, Voorsterweg 31, Marknesse, 8316 PR, Netherlands

## ARTICLE INFO

### Article history:

Received 23 August 2021

Received in revised form 9 November 2021

Accepted 30 November 2021

Available online 9 December 2021

### Keywords:

Piezoelectric actuators

Self-heating

Thermal vacuum

Power dissipation

## ABSTRACT

Piezoelectric actuators are a very attractive technology for active optics mechanisms in space applications due to their very high precision and reliability. However, self-heating of these actuators may limit their use in space or under high loads, due to the limited ability to evacuate heat. Test procedures that reproduce the operational conditions of these actuators are important to check these operational limits. Here an effort to characterise the thermal emission of pre-stressed piezoelectric actuators in operation is presented. The technique allows direct measurement of the power dissipated by the test item via the control of the different heat transfer mechanisms, using the fall in power provided as measure of power dissipated by the actuators, instead of relying on direct temperature sensors. This allows the construction of a thermal model with a dissipation term readily integrated in system-level modelling to account for the dissipated heat of the piezo. The technique may also be applied to other piezo low power applications in the order of 1 W of thermal emission, and is adaptable to emulate the boundary conditions encountered in operations.

© 2021 The Author(s). Published by Elsevier B.V.  
CC BY 4.0

## 1. Introduction

### 1.1. Piezoactuators in space instrumentation

Spaceborne instrumentation is essential for monitoring our Earth environment and observing distant objects in the universe. The demand for higher quality imaging drives the design of larger instruments which can achieve higher resolution at the diffraction limit. This demand necessitates larger and more capable observatories than currently available at comparable stowed volumes. One way to achieve this is the use of segmented aperture telescopes, which require precise positioning of their optical elements relative to each other [24]. In other cases, instruments which do not have segmented apertures may also require actuation of their focal plane assembly, or of other intermediate elements in the optical path. Examples of these latter elements are deformable mirrors, and fast steering mirrors.

Advanced future space observatories will integrate many active optical elements whose actuation must be very precise to comply with misalignment requirements. In prior instruments, the technology of choice has been the stepper motor combined with a

reduction gearbox and a flexure amplifier, such as the case of the James Webb Space Telescope (JWST) [26]. In current and future instruments, it is possible that some of these actuation stages are powered by pre-stressed piezoelectric actuators due to their simpler mechanical characteristics, high stiffness, fast response and high repeatability [25]. Losses present in these materials, as they convert electrical power into motion during repetitive operation cause them to warm up, a phenomenon referred to as self-heating [21].

Piezoelectric actuators exhibit complex behaviour from a control standpoint, characterised by strong field-polarization hysteresis [29]. In addition, piezoelectric materials are subject to creep and saturation [1]. Even so, piezoelectric actuators are capable of reaching resolutions in the order of one nanometre, provided accurate control can be designed. Several approaches are described in the literature for drive and control of these actuators [11,17].

### 1.2. Self-heating of Piezoelectric Actuators

Piezoelectric ceramics are classified in soft and hard [4]. Hard piezoelectric materials tend to have smaller piezoelectric constants. They are used for applications where small displacements and high frequencies are needed. Typical examples are ultrasonic transducers. Soft piezoelectric materials have larger piezoelectric constants, which produce larger strokes. This is advantageous for actuators which work at lower frequencies. The latter type of material is of

\* Corresponding author.

E-mail address: [v.m.villalbacorbacho@tudelft.nl](mailto:v.m.villalbacorbacho@tudelft.nl) (V. Villalba Corbacho).

interest for this research since the application is a precision actuator. In addition, piezoelectric actuators may operate in linear mode, or in bending mode, and embedded in a wide variety of motion amplifiers [4,12]. In this paper, the focus is given to linear-mode actuators constructed out of piezoceramics. These actuators have a smaller range of motion with respect to stepping bending mode actuators, but have much higher stiffness and blocked force. The linear actuators used in applications where high precision is needed are pre-stressed by a frame, which reduces stick-slip behaviour at the interface between the mechanism and the actuator and provides a standard interface. Fig. 1 shows a linear pre-stressed actuator that was used in the tests of this study.

Self-heating of piezoactuators may be a challenge both in optical and thermo-mechanical terms. Even before complete thermal failure of the actuator, additional heat may disturb measurements in thermal infrared (TIR) instruments. Heat leaking from the actuator may cause misalignment due to thermal expansion of either the actuator or its surroundings. In addition, self-heating has been identified as a potential source of runaway thermal failure due to increased current draw at high temperatures [20]. Self-heating also changes the electrical properties of the actuators, which are sensitive to temperature, and need to be compensated [19,28]. Materials for high thermal stability may be designed, but the temperature dependence is difficult to remove [9,10]. Weaver et al. reviewed several methods of characterization of piezoelectric parameters in high temperature materials [27]. Temperature measurement as a control parameter has been proposed to compensate for

temperature dependence of actuator capacitance [5]. Thermal cycling, which can be caused by self-heating, has been identified as a factor in adhesive bonding failure in piezoelectric sensors [2]. Tests addressing this phenomenon are important to qualify the system and build a reliable thermal model of the mechanism.

Prior experiments on the self-heating effect of piezoelectric actuators have relied on a transient analysis of the actuator response [18,22,31]. In this method, the actuator is initially inactive and upon activation with a given frequency and amplitude, self heating begins. Pritchard et al [14] inverted the approach to calculate heat dissipation of multi-layer actuators. If temperature is plotted against time in this configuration, the response is analogous to a step response of a first order system. The exact parameters of the decaying exponential solution to the transient are fitted via a parameter  $k_T$  which models the system dynamics. This includes the conductive, radiative and convective couplings of the actuator to its environment and allows a good fit of the behaviour. However, such a study does not allow direct computation of the generated heat flow. Moreover,  $k_T$  is a fitting parameter which is difficult to trace back to first principles if the thermal couplings to the environment are not well characterised. In addition, these models are difficult to integrate into system-level thermal models where boundary conditions are complex.

In this study, the goal of the test setup is to observe the self-heating in a more direct manner, without relying on such transient fitting techniques. The observation principle here is based on steady state thermal equilibrium between the test item and its environment. Another measurement procedure relying on steady-state measurements was carried out by Quattrocchi et al. [15] but the authors do not calculate heat production directly. In this test setup, a more thorough control of thermal boundary conditions is also sought. The objective in the test setup design was to create a single possible thermal path for heat to flow from the actuators into a cold reservoir. Prior to actuator self heating, the setup will be dissipating a known amount of heat with the main thermal path at a constant temperature. The temperature of this path will remain under control once the actuator is switched on. Therefore, in order to keep steady state thermal equilibrium, the known dissipated power will fall by the same amount as the actuator dissipates.

## 2. Modeling self-heating

Self-heating has been studied previously in the context of fuel injectors by Senousy et al. [18] and in general by Ronkanen et al. [16]. Khan et al. [6] developed a constitutive model to predict temperature rise and polarization hysteresis. They obtained good results in polarization hysteresis, but temperature rise was not well predicted experimentally, which the authors attribute to deficient heat transfer control to establish boundary conditions. The factors influencing self-heating were also compiled by Stewart and Cain [20] and can be summarised as:

- Voltage or electric field
- Excitation frequency
- Temperature
- External load
- Actuator size
- Duty cycle

The two widely cited contributions to overall self-heating are strain losses and dielectric losses [20]. Uchino and Hirose add another contribution solely related to the piezoelectric effect [21,22]. Strain losses are caused by internal friction in the actuator. This friction can appear at grain boundaries in polycrystalline materials,

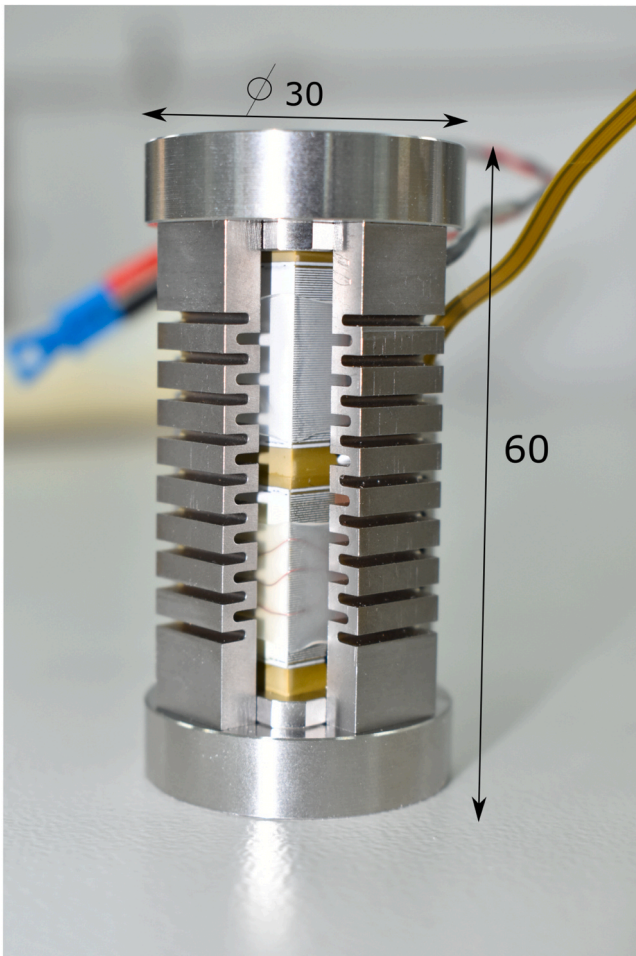


Fig. 1. Pre-stressed actuator, a test item for this study.

or at the interface with electrodes in thin-film deposited materials. [8] The work performed by the load to overcome this internal friction is lost as heat. The estimation of dielectric losses is further compounded by the temperature dependence of the piezoelectric's dielectric constant. For operations close to the resonant frequency of the actuator, strain losses are dominant over dielectric losses. Dielectric losses dominate in case of frequencies far from resonance [20].

Voltage and electric field may be used interchangeably when referring to the experiment control parameters, although electric field is a more rigorous reference to the fundamental principles of piezoelectric actuators. Multi-layer actuators are operated in voltage, and the corresponding electric field found in the layers of the actuators is computed as the applied voltage over the layer thickness.

The effect of external loads was investigated by Li et al. [7], who concluded that pre-load has a very modest effect on heat production. This load was investigated with a pre-loading spring. Actuator size has been identified as a relevant parameter when studying piezoelectric materials because as cross sectional area increases, the ratio area to volume also increases and the ability to evacuate heat on the edges of the actuator decreases, resulting in higher temperature setpoints.

Heat transfer in this context is described by the classical triad of heat transfer mechanisms: convection, radiation and conduction. However, convection is difficult to predict and, space applications, mostly absent. The focus is in vacuum conditions, which severely limits the heat evacuation of the piezoelectric materials and therefore reduces their operational space.

### 3. Experimental setup

The goal is to measure self-heating power of piezoelectric actuators. Based on information provided by the manufacturer, the power dissipated would depend on the frequency and amplitude of actuation, which for limit cases would be in the order of 5 W. The experimental setup's achievable resolution using this technique was not characterised, but the smallest detectable heat fluxes were desired to be in the order of 10 mW. The test items were three PPA40XL actuators manufactured by Cedrat Technologies, although only one was tested inside the vacuum chamber, whilst all three were subjected to additional tests.

#### 3.1. Description

The test item is placed in a thermal vacuum (TV) chamber to remove natural convection between the actuator and the environment. TV describes here a vacuum chamber with a shroud which incorporates thermal control, which allows manipulation of the radiative thermal environment of the sample. A schematic of the system can be found in Fig. 2. The complete setup consists of:

- Test item, a pre-stressed piezoelectric actuator
- Constrained thermal path
- Thermal control and measurement systems
- Piezoelectric control electronics
- Mechanical load simulator

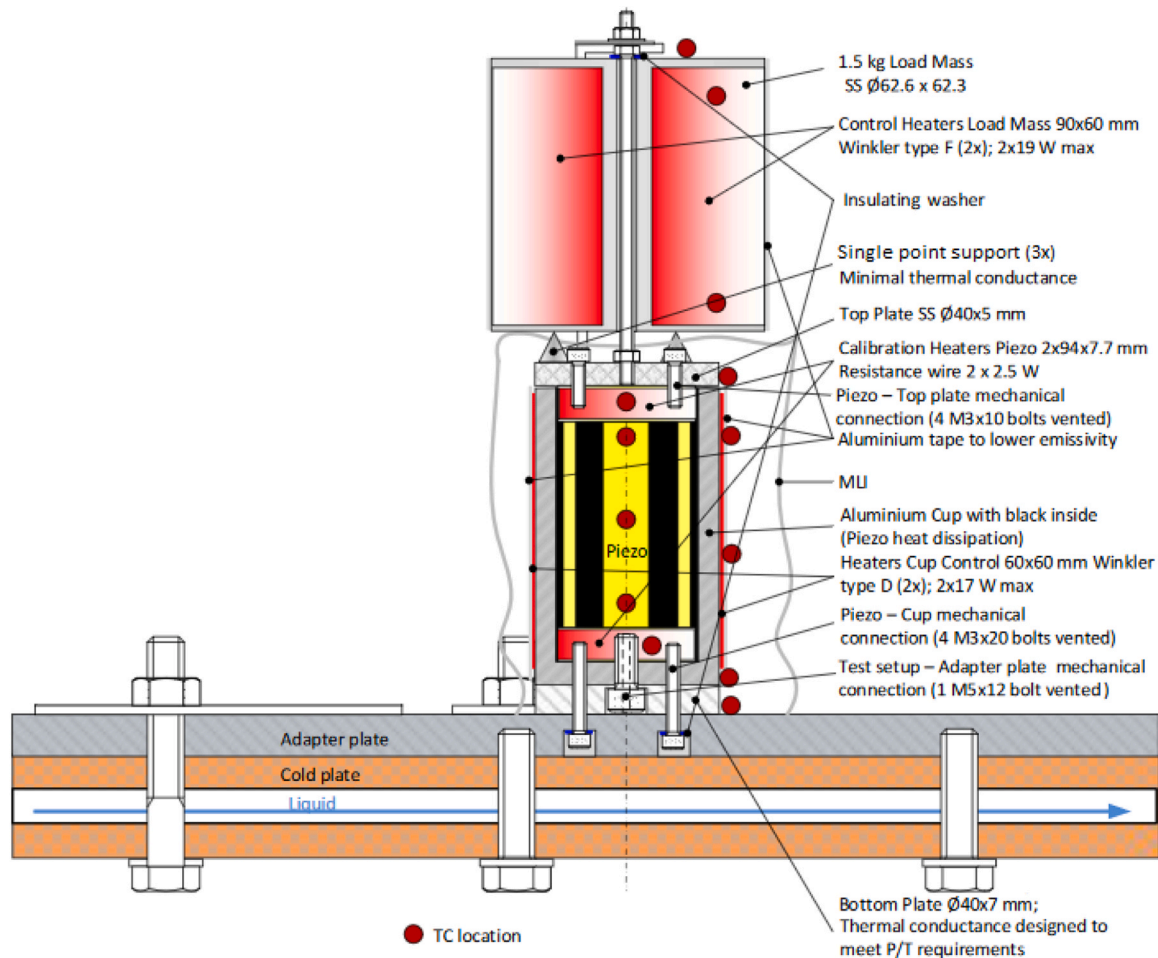


Fig. 2. Schematic of test setup in thermal vacuum.

**Table 1**  
Characteristics of the test actuator.

Property	Value
Length	60 mm
Cross section	30x30 mm
Capacitance	20 $\mu\text{F}$
Layer thickness	100 $\mu\text{m}$
Nominal preload	20 MPa
Temperature range	-40–80°C
Coupling mode	33

During the test campaign, points of improvement of the setup were noted. Thermal fluxes could be characterised with a resolution in the order of 60 mW as demonstrated during the calibration procedure. This is likely sufficient for most applications, but processes with very small heat fluxes may not be characterised without modifications. The main characteristics of the test items are summarised in Table 1.

The thermal control and measurement system is placed around the actuator. It consists of a cold plate cooled with a working fluid at a fixed temperature. The temperature is controlled via a reservoir of gas nitrogen evaporated through a liquid nitrogen pool. The gas flow passes through a heater channel which brings its temperature to the desired level. In this way, thermal stability of the cold reservoir in the order of 0.05 K was maintained for three hours. Stability was only compromised during operations to re-fill liquid nitrogen tanks for cooling for the gas nitrogen, which was taken into account during testing operations. Due to the good conductive coupling between the actuator and the cold plate, maintaining temperature homogeneity is critical, as a change in the temperatures within the thermal path changes the power needed for steady state operation. Possible improvements to the thermal stability of the setup are liquid coolants, or a two-phase cooling fluid, taking advantage of the larger heat capacity of these options to attenuate local fluctuations in the temperature.

The actuator is placed within an aluminum cup which is coated black to maximise its radiative coupling to the actuator. The cup is wrapped with low emissivity tape and multi-layer insulation (MLI) to minimise radiative losses to the environment, which forces all heat produced to go to the cold plate. Guard heaters at the mass at the top of the actuator match the temperature measured at the actuator, so as to net zero heat transfer on that side. The heat leak through the cup to the environment determines the achievable resolution of the setup. A calibration heater is integrated on the actuator to dissipate a controlled amount of heat to characterise the setup, but this is not used during measurements. A schematic of the test setup is shown in Fig. 2. The actuator with copper wire heaters integrated is shown in Fig. 3.

The types of wires needed in this setup are the lead cables for the piezoelectric actuator and calibration heaters to function, and the thermocouple wires. Thermocouples are directly glued to the sample. Wires which go inside of the cup is places do not require additional insulation, as free heat transfer within the cup is desired. Those which are in thermally insulated parts are covered with reflective tape to minimise radiation losses. The wires are pulled into the cup through a small gap which is also fit with MLI. Since the wires are small compared to the overall size of the setup, heat leakage through them is neglected.

The piezoelectric control electronics consist of a waveform generator controlled by a desktop computer programmed in LabView. Signals produced by the waveform generator are amplified with a Cedrat LA-75C linear piezoamplifier and sent to the actuator. Strain gauges attached to the actuator make it possible to probe the behaviour of the actuator in displacements, which is interesting to control for the motion amplitude when analyzing the data.

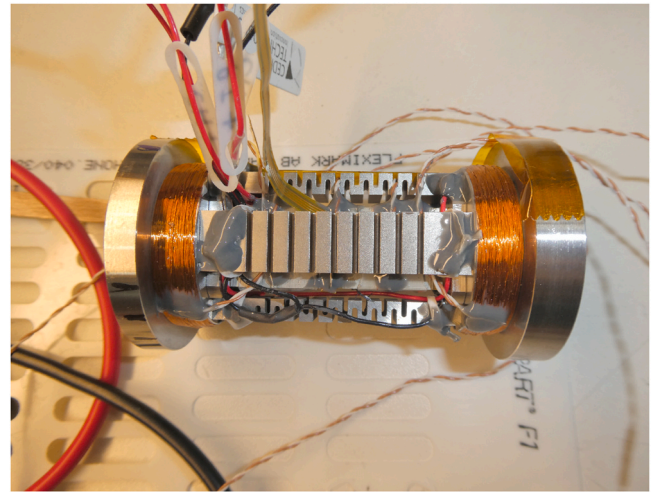


**Fig. 3.** Picture of actuator wrapped in copper wire as integrated heater for characterization purposes.

Inertial loads are simulated by placing a stainless steel weight, which is thermally isolated but mechanically coupled to the actuator. In prior research, load was indicated to be a factor reducing thermal dissipation for a voltage-controlled actuator [16]. This however was done without displacement data, and the expectation is that increasing the load would decrease range of motion. In the case of the pre-stressed actuator, a load level is always present on the actuator. The mass simulation added to it allows calculating the sensitivity of heat dissipation to higher inertial loads.

In the TV chamber, frequency and amplitude can be changed without opening the chamber, which allows batches of tests to be carried out in sequence and minimise total time testing. Controlling the temperature of the cold plate to provide a different temperature setpoint to the actuator can also be done without opening the chamber, but requires manual operation of the pumps. Finally, changing the loads on the actuator or the actuator itself are more intrusive operations which require opening the vacuum chamber. This was avoided because the vacuum chamber requires a complete day to return to operation once the vacuum is lost Fig. 4 shows the open TV chamber with its thermal control equipment and control electronics.

### 3.2. Limitations of the test setup and data treatment

In order to yield high resolution in power production, the thermal path between the actuator's environment needs to be closed to external losses. In this way, all heat produced by the actuator can be measured. Several well-known practices have been used to limit these heat leaks in the setup, though it is difficult to remove them entirely. Radiative losses from the cup to the shroud are reduced by wrapping the setup in MLI. Another important potential heat leak is the mass simulator on the top of the actuator. This is coupled with the actuator via a screw in the center supported by point contact. The bolted connections between the actuator and the mass are further insulated by the use of thermal washers with poor thermal conduction.

The losses are further reduced by matching the temperatures in their thermal paths. The shroud of the vacuum chamber is set to follow the temperatures of the cup to further minimise heat leak through the cup. The mass is equipped with guard heaters, controlled to match the temperature of the top of the actuator. Note these two temperatures do not necessarily match in transient due to the mass thermal controller is not tuned to closely follow its target, only to reach it in steady state.



Fig. 4. Open vacuum chamber and control and measurement equipment.

Another major source of error in the measurements is the fluctuation in thermal homogeneity of the adapter plate that acts as interface between the cold sink and the test setup. The temperature of this plate is controlled with the feedback of a thermocouple with another to spare. The latter thermocouple was expected to have a constant offset with the former. However, whilst the controlled thermocouple is stable to within  $\pm 20$  mK, the spare thermocouple registers slow fluctuations over several hours in the order of  $\pm 0.1$  K, indicating thermal inhomogeneity in this interface. This is significant due to the good conductive coupling between the actuator and the cold plate, as these fluctuations also cause large fluctuations (order of hundreds of milliwatts) in the power measured. A better iteration of this test setup would solve this problem by adding more thermocouples in this critical heat path and tuning the control to keep all of them equally stable. The current iteration the test setup is not capable of fully characterising this behaviour, which introduces measurement uncertainty.

During the test campaign, points of improvement of the setup were noted. Thermal fluxes could be detected with a resolution in the order of 60 mW as demonstrated during the calibration procedure, but these results cannot be trusted to be accurate if the stability of the cold plate is compromised. This is likely sufficient for most applications, but processes with very small heat fluxes (order of 10 mW) may not be characterised without modifications. Note that temperature rise can be observed without noticeable increase in observed power dissipation with the instrumentation.

## 4. Results

### 4.1. Calibration

The objective of the calibration runs is characterising the measurement procedure. A known amount of power is dissipated in heaters attached to the hubs of the pre-loading structure of the piezoactuator. The controller keeps the temperature of the control thermocouple unaltered by reducing the heat it releases into the setup. Since all the heat fluxes are known in this case, a discrepancy between the measured and the introduced powers indicates a heat leak or another measurement problem.

Data from this calibration run show that the setup underestimates power introduced via this method due to heat leaks. The primary heat leaks causing this were described in subsection 3.2. The largest influence on the readings was the instability of the cold plate. The trend of this instability over a day of testing is diminishing temperature with time each day, although the trend reverses by the end of a test period, corresponding also to an decrease in power to keep temperatures stable. This confirms that the power measurement swings are related to this phenomenon.

Typical steady-state error of the temperature control is in the order of 0.05 K. The heat leak though the MLI was estimated to be negligible compared to the two main heat leaks. The final heat leak is the remnant transient, which can be estimated knowing the mass and materials of the setup per experiment.

Knowing the temperatures of the cold sink, the mass and the shroud, a calibration equation is proposed to turn raw power measurement data into corrected power measurements:

$$P_{Cor} = P_{Raw} + C_{Sink} \Delta T_{Sink} + C_{Mass} \Delta T_{Mass} + C'_{Trans} \frac{\Delta T_{ACT}}{\Delta t} \quad (1)$$

This method, applied to the calibration runs, shows that once these heat leaks are corrected, the setup produces good measurements of heat. However, later tests with the piezoactuators active at low electric field magnitudes show that measurements below the 150 mW threshold are not reliable. Fig. 5 shows the uncorrected and corrected results when dissipating a known quantity of heat into the system. The constants in Equation 1 were found by minimising the relative error between the corrected measurement and the known quantities of heat dissipated in the different tests.

The same procedure was followed with the tests performed in cold conditions. These constants are sensitive to large temperature changes, because thermal expansion of the interfaces in the setup alters their conductive properties [3]. Therefore, correction constants need to be found for each temperature setpoint with this technique. The temperature control of the interface, however, guarantees that given a global setpoint, the interface is not affected by the heat generation of the process being measured Table 2 shows the values of the correction constants applied in the two temperature setpoints.

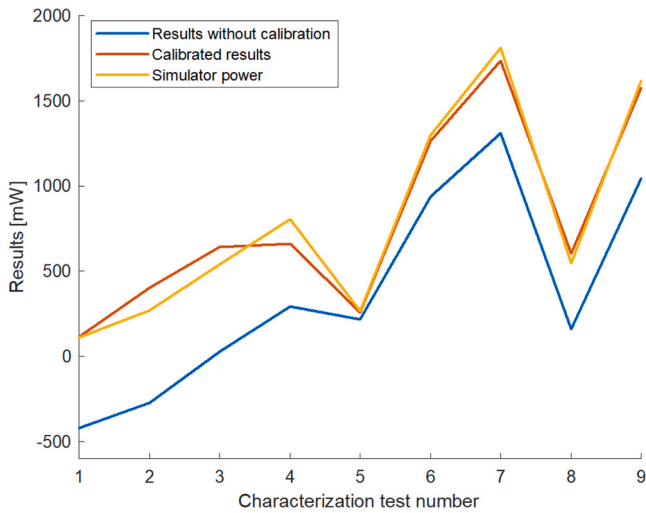


Fig. 5. Uncorrected results of the setup characterization runs. The x axis only shows the test number, simulator power in each test is decided by the operator.

Table 2  
Correction factors for the two TV test conditions.

	$C_{Sink}$ [mW/K]	$C_{Mass}$ [mW/K]	$C_{Transient}$ [mW/sK]
$T_{Sink} = 0^{\circ}C$	2479	383.8	136.4
$T_{Sink} = -40^{\circ}C$	2787	212.1	348

4.2. Power measurement

The real power measurements were carried out in the TV chamber. The principle of measurement was proven to work, but its resolving power is limited at low power dissipations in the order of 500 mW. At high dissipation, the boundary condition control limits the amount of heat that can be effectively evacuated from the PZT stack. This limitation in heat flow causes a rise in the internal temperature of the piezoelectric stack in the actuator at high power dissipation. Tests were interrupted by a safety trigger when temperatures rose to 80°C. This limits the space of frequency and amplitude that can be probed with this setup. The limits to this space were found via trial and error. All tests were performed with sinusoidal excitation. The defining characteristics of the inputs used are summarised in Table 3.

Figs. 6 and 7 show the corrected measurements from the piezoelectric actuators as a function of frequency and amplitude respectively. The error bars represent the magnitude of the correction factors applied to the setup as a measure of uncertainty. Note that the error bars may reach negative values, but this would not make physical sense.

Table 3  
Input characteristics for the different tests.

Actuator 1 TV	Frequency [Hz]	Voltage [V]
	50	42.5
	20	85
	5	170
	100	42.5
	150	42.5
	50	85
	20	170
	100	85
	150	85
	20	127.5
	40	170
	190	21.5
	190	21.5

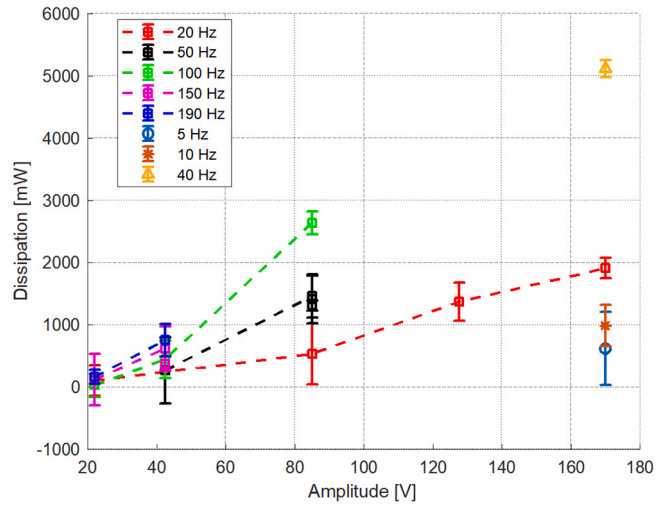


Fig. 6. Measured thermal dissipation as a function of amplitude for different excitation frequencies.

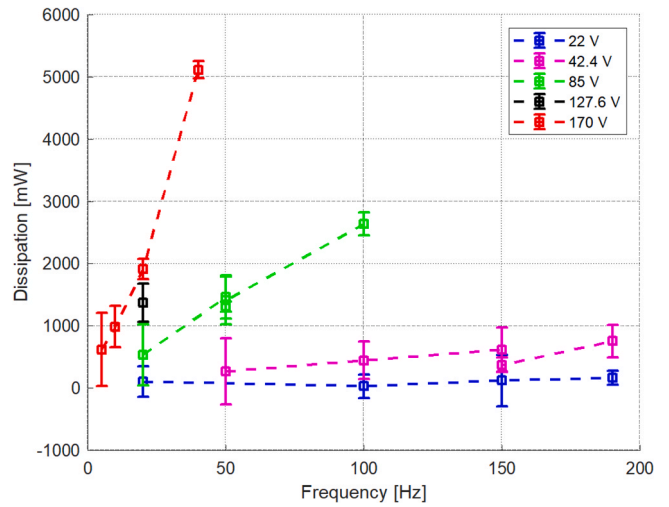


Fig. 7. Measured thermal dissipation as a function of frequency for different excitation amplitudes.

In this setup, the amplifier output was verified to be according to manufacturer specification. However, there was no way of recording those values as the tests were progressing. This was done with the actuators outside of the vacuum, as described in the following section.

The cold plate and shroud were brought to a cold setpoint at -40°C. The test was repeated for a reduced set of actuation parameters. The expectation was that dissipation at colder temperature setpoints would be significantly smaller than at ambient because such behaviour has been reported in the literature. However, in this study there is no significant evidence as to the effect of temperature in the power dissipation in this temperature range. Table 4 shows final results for both temperature settings.

Table 4  
Comparison of results at 0°C and -40°C for different settings.

Test parameters	0°C setpoint [mW]	-40°C setpoint [mW]
50 Hz / 85 V	1461.4 / 1311 / 1408.6	1340
100 Hz / 85 V	2639.7	2742.3
20 Hz / 170 V	1909.9	2068.8



Fig. 8. Setup outside of vacuum.

4.3. Transient open air test

An additional test was performed outside of the vacuum chamber with actuators of the same model and manufacturer. The experimental procedure presented herein is difficult to set up and to run, so it was not done for the several actuators. In order to have confidence that the actuators behave in similar fashion, a simpler setup with no vacuum chamber was prepared. A glass cover isolates the actuator stack from air currents in the lab. The cold plate is kept at 15°C via a cooling loop of glycol and water. This setup can be seen in Fig. 8.

In this test, the output voltage of the amplifier and the voltage prior to a shunt resistor are recorded by an oscilloscope. The instantaneous power consumed by the actuator can be modeled as:

$$P(t) = (V_{amp}(t) - V_{shunt}(t)) * V_{shunt}(t) / R_{shunt} \tag{2}$$

Where  $V_{amp}$  and  $V_{shunt}$  are the voltages at the amplifier output and across the shunt resistor and  $R_{shunt}$  is the resistance of the shunt. These signals were multiplied in time domain to obtain instantaneous power and then averaged over 5 cycles to obtain the power reading. The measured signal  $V_{amp}(t)$  includes a DC offset as a result of the amplifier not delivering a zero-average sine wave. This DC component is filtered by the actuator due to its capacitive nature of the actuator, which is seen on DC as an open circuit. Therefore, no current can flow on DC and no power is consumed. More precisely, in DC conditions, there can be some current leakage through any real material, which can be seen in the models presented by Paganelli et al. [13]. In this application, however, this effect was too small to be

Table 5 Characteristics of the sine waves used in out of vacuum (OOV) tests.

Actuator 1/2/3 OOV	Frequency [Hz]	Voltage [V]
	50	42.5
	20	85
	5	170
	100	42.5
	150	42.5
	50	85
	20	170
	100	85
	150	85
	40	170

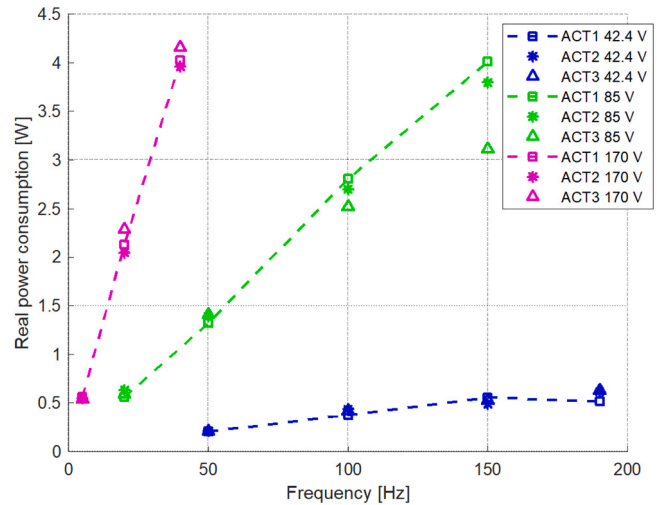


Fig. 9. Power consumption results of the different actuators tested outside of the vacuum.

detected. Other models, such as proposed by Zhang et al. do not consider this potential leakage in DC at all [30]. Table 5, Fig. 9.

Table 5 shows the frequency and amplitudes use for testing on this setup. The results of real power consumption are shown in Fig. 9. These values show agreement with the results presented in the TV test as shown in Fig. 10. A notable exception is the maximum dissipation case in both, which is a setting of 40 Hz at 170 V. In this case, dissipation directly measured is significantly larger in TV. This

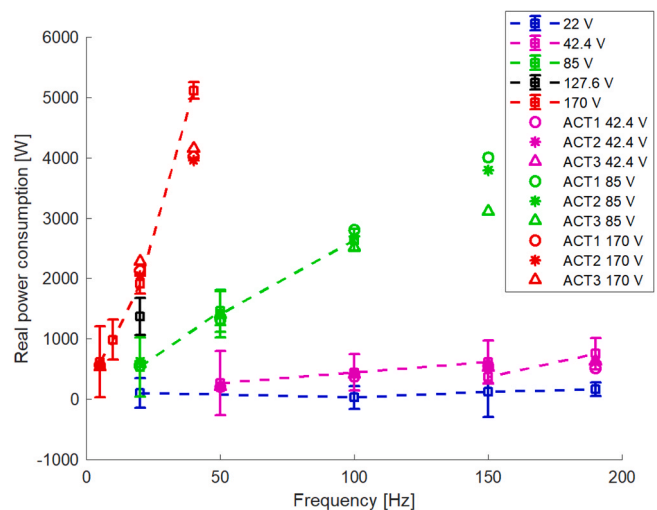


Fig. 10. Lost power results from the tests carried out inside and outside vacuum. Datapoints joined with discontinuous lines represent TV tests, the rest are OOV tests.



is likely a result of the higher actuator temperature reached in TV, as it is not possible to evacuate as much heat as in the presence of air. This effect was not present at cold temperatures, but it is, as previously mentioned, well established in literature.

## 5. Conclusions

The described measurement method for heat dissipation is capable of producing a dissipation profile for piezoelectric actuators or other types of heat generating low power test items. The measurement principle has been demonstrated and described in the paper, but several challenges remain to improve its resolution, and more importantly its repeatability. Measurements from this method have been used to compare dissipation in different temperature setpoints, and can be adapted to better reflect the boundary conditions encountered in real operations. The method's current shortcomings have been analysed and mitigation strategies have been proposed for future iterations.

## 6. Future work

The technique described in this paper was novel and there are several changes which can improve accuracy and repeatability of direct power measurements for piezoactuators and other low-power electrical components. These were deemed unnecessary during the design of the experiment, which in hindsight should have been part of it. Quantitative measurements of current system repeatability were not executed, which was a flaw in the test protocol, but repeatability is expected to improve with the proposed changes.

One challenge in the data analysis of the setting was the erratic behaviour of the main thermal path through the adapter plate. Even though stability was better than 0.1 K/h, this is not sufficient to resolve low power dissipation without correcting for thermal drift of the cold plate. In addition, the fact that only two thermocouples monitored this thermal path meant there could be unexplored contact dynamics at the interface which cannot be accounted for with the current sensing equipment. In order to address this problem, a more thermally conductive material could be used to construct this part of the setup, with the goal of reducing zonal differences. In addition, more thermocouples are needed to fully characterise the complex bolted interface and design the control strategy accordingly.

Thermal stability can also be improved by changing cooling technology. Gas nitrogen is safe to use in the vacuum chamber even if a leak occurs. Other possibilities which could perform better are a glycol bath, or more adequately, a two-phase cooling loop such as described on [23]. However these are more complex and less safe alternatives in case of leakage in the vacuum chamber.

## CRedit authorship contribution statement

**Víctor Villalba:** Conceptualization, Methodology, Validation, Analysis, Investigation, Visualization, Writing – original draft. **Johannes van Es:** Conceptualization, Methodology, Validation, Resources, Writing – editing & review. **Hans Kuiper:** Conceptualization, Resources, Writing – editing & review, Supervision, Project administration, Funding acquisition. **Eberhard Gill:** Resources, Supervision, Writing – editing & review, Project administration.

## Declaration of Competing Interest

The authors declare that they have no known competing financial interests or personal relationships that could have appeared to influence the work reported in this paper.

## Acknowledgements

The authors would like to acknowledge the contributions of Adry van Vliet, Wubbo de Grave and Aswin Pauw to the test setup.

## References

- [1] Mohd Hafiz Abdul Satar, Ahmad Firdaus Murad, Ahmad Zhafran Ahmad Mazlan, Characterization of piezoelectric patch material with hysteresis, saturation, creep, and vibration nonlinearity effects and its application to the active vibration suppression for cantilever beam, *JVC/J. Vib. Control* (2020) 1–14.
- [2] J.L. Blackshire, S. Martin, A. Cooney, Characterization and modeling of bonded piezoelectric sensor performance and durability in simulated aircraft environments, *Proc. 3rd Eur. Workshop - Struct. Health Monit. 2006 1694* (2006) (2006) 283–289.
- [3] M.G. Cooper, B.B. Mikic, M.M. Yovanovich, Thermal contact conductance, *Int. J. Heat Mass Transf.* 12 (3) (1969) 279–300.
- [4] Xiangyu Gao, Jikun Yang, Jingen Wu, Xudong Xin, Zhanmiao Li, Xiaoting Yuan, Xinyi Shen, Shuxiang Dong, Piezoelectric actuators and motors: materials, designs, and applications, *Adv. Mater. Technol.* 5 (1) (2020) 1–26.
- [5] Mohammad Islam, Rudolf Seethaler, David Mumford, Real time temperature measurement for multilayered piezoelectric stack actuators, *Canadian Conference on Electrical and Computer Engineering, IEEE, 2011*, pp. 001194–001197.
- [6] Kamran A. Khan, Anastasia H. Muliana, Hassene Ben Atitallah, Zoubeida Ounaies, Time-dependent and energy dissipation effects on the electro-mechanical response of PZTs, *Mech. Mater.* 102 (2016) 74–89.
- [7] F.X. Li, R.K.N.D. Rajapakse, D. Mumford, M. Gadala, Quasi-static thermo-electro-mechanical behaviour of piezoelectric stack actuators, *Smart Mater. Struct.* 17 (1) (2008).
- [8] Gang Liu, Shujun Zhang, Wenhua Jiang, Wenwu Cao, Losses in ferroelectric materials, *Mater. Sci. Eng. R Rep.* 89 (2015) 1–48.
- [9] Xiaolian Liu, Guodong Wang, Meiya Li, Jianguo Chen, Shuxiang Dong, Zhongqiang Hu, Development of hard high-temperature piezoelectric ceramics for actuator applications, *J. Mater. Sci. Mater. Electron.* 26 (12) (2015) 9350–9354.
- [10] Xu Lu, Liang Wang, Li Jin, Qingyuan Hu, Ye Tian, Lei Hou, Kun Yu, Lin Zhang, Xiaoyong Wei, Yan Yan, Gang Liu, Ultra-low hysteresis electrostrictive strain with high thermal stability in Bi(Li<sub>0.5</sub>Nb<sub>0.5</sub>)O<sub>3</sub>-modified BaTiO<sub>3</sub> lead-free ferroelectrics, *J. Alloy. Compd.* 753 (2018) 558–565.
- [11] J. Minase, T.F. Lu, B. Cazzolato, S. Grainger, A review, supported by experimental results, of voltage, charge and capacitor insertion method for driving piezoelectric actuators, *Precis. Eng.* 34 (4) (2010) 692–700.
- [12] S. Mohith, Adithya R. Upadhy, Karanth P. Navin, S.M. Kulkarni, Muralidhara Rao, Recent trends in piezoelectric actuators for precision motion and their applications: a review, *Smart Mater. Struct.* 30 (1) (2021).
- [13] Rudi P. Paganelli, Aldo Romani, Alessandro Golfarelli, Michele Magi, Enrico Sangiorgi, Marco Tartagni, Modeling and characterization of piezoelectric transducers by means of scattering parameters. Part I: theory, *Sens. Actuators A Phys.* 160 (1–2) (2010) 9–18.
- [14] J. Pritchard, R. Ramesh, C.R. Bowen, Time-temperature profiles of multi-layer actuators, *Sens. Actuators A Phys.* 115 (1) (2004) 140–145.
- [15] Antonino Quattrocchi, Fabrizio Freni, Roberto Montanini, Self-heat generation of embedded piezoceramic patches used for fabrication of smart materials, *Sens. Actuators A Phys.* 280 (2018) 513–520.
- [16] Pekka Ronkanen, Pasi Kallio, Matti Viikko, and Heikki N. Koivo. Self heating of piezoelectric actuators: Measurement and compensation. *Proceedings of the 2004 International Symposium on Micro-NanoMechatronics and Human Science*, 313–318, 2004.
- [17] D. V. Sabarianand, P. Karthikeyan, and T. Muthuramalingam. A review on control strategies for compensation of hysteresis and creep on piezoelectric actuators based micro systems, 6, 2020.
- [18] M.S. Senousy, R.K.N.D. Rajapakse, D. Mumford, M.S. Gadala, Self-heat generation in piezoelectric stack actuators used in fuel injectors, *Smart Mater. Struct.* 18 (4) (2009).
- [19] Siripong Somwan, Apichart Limpichaipanit, Athipong Ngamjarujana, Effect of temperature on loss mechanism of 0.7PMN–0.3PZT ceramics, *Sens. Actuators, A Phys.* 236 (1) (2015) 19–24.
- [20] Mark Stewart, Markys G. Cain, Measurement and modelling of self-heating in piezoelectric materials and devices, in: Markys G. Cain (Ed.), *Characterisation of Ferroelectric Bulk Materials and Thin Films*, chapter 7, Springer, 2014.
- [21] K. Uchino, *High-Power Piezoelectrics and Loss Mechanisms*. In *Advanced Piezoelectric Materials - Science and Technology* (2nd Edition), chapter 17. 2nd edition, 2017.
- [22] Kenji Uchino, Seiji Hirose, Loss mechanisms in piezoelectrics: how to, *IEEE Trans. Ultrason.* 48 (1) (2001) 307–321.
- [23] Henk Jan van Gerner, Robin Bolder, Johannes van Es, Transient modelling of pumped two-phase cooling systems: comparison between experiment and simulation, *47th Int. Conf. Environ. Syst.*, Number July (2017) 1–15 (Charleston).
- [24] V. Villalba, H. Kuiper, E. Gill, Review on thermal and mechanical challenges in the development of deployable space optics, *J. Astron. Telesc. Instrum. Syst.* 6 (1) (2020).
- [25] Víctor Villalba, Sean Pepper, Hans Kuiper, Eberhard Gill, Development process of an active optics mechanism for a deployable space telescope, *Submit. Precis. Eng. Rev.* (2021).

- [26] M. Warden Robert, Cryogenic nano-actuator for JWST, 38th Aerosp. Mech. Symp. (2006).
- [27] P.M. Weaver, T. Stevenson, T. Quast, G. Bartl, T. Schmitz-Kempen, P. Woolliams, A. Blumfield, M. Stewart, M.G. Cain, High temperature measurement and characterisation of piezoelectric properties, *J. Mater. Sci. Mater. Electron.* 26 (12) (2015) 9268–9278.
- [28] Juhyun Yoo, Jongmyung Im, Inho Im, Physical characteristics of  $(1-x)(\text{Na,K})(\text{Nb,Sb})\text{O}_3$ - $(\text{Bi,Na})\text{ZrO}_3$ - $x\text{BaZrO}_3$  ceramics for piezoelectric actuator, *Trans. Electr. Electron. Mater.* 21 (5) (2020) 477–481.
- [29] Yunhe Yu, Nagi Naganathan, Rao Dukkipati, Preisach modeling of hysteresis for piezoceramic actuator system, *Mech. Mach. Theory* 37 (1) (2002) 49–59.
- [30] Yangkun Zhang, Tien Fu Lu, Yuxin Peng, Three-port equivalent circuit of multilayer piezoelectric stack, *Sens. Actuators A Phys.* 236 (2015) 92–97.
- [31] Jiheui Zheng, Sadayuki Takahashi, Shoko Yoshikawa, Kenji Uchino, Heat generation in multilayer piezoelectric actuators, *J. Am. Ceram. Soc.* 79 (12) (1996) 3193–3198.

Victor Villalba, MSc, is a PhD candidate at the department of Space Engineering of the Delft University of Technology. He holds a bachelor's degree in Aerospace Engineering from the University of Seville and an MSc in Space Science and Technology from Cranfield University and the Lulea University of technology. His research interest is in

stable structures and actuation mechanisms for stabilization of deployable space telescopes.

Johannes van Es is a senior research manager and lead system engineer at the National Aerospace Laboratory (NLR). He has been a researcher in satellite thermal control and thermal engineering for over 20 years. He holds an MSc in Engineering Physics from the University of Twente.

Dr. ir. Hans Kuiper is an Assistant Professor at the department of Space Engineering, Delft University of Technology. Previously he held technical positions at the Dutch hi-tech industry for more than 30 years. He holds an MSc in Applied Physics from the Eindhoven University of Technology and a PhD in Space Systems Engineering from the Delft University of Technology. His research interest is in the systems engineering of spaceborne optical instruments.

Prof. dr. Eberhard Gill is the head of the Space Systems Engineering section at the Delft University of Technology. His interest is in the design and engineering of distributed and miniaturized space systems. He holds a PhD in theoretical astrophysics from the University of Tübingen and an MSc in Space Systems engineering from the Delft University of Technology.